小児科診療〔第67巻・第8号〕別刷

2004年8月1日発行

発行所 株式会社 診断と治療社

特集　小児科医が知っておきたい眼科疾患

遺　伝

小須賀基通　奥山虎之　国立成育医療センター遺伝診療科

要旨

近年の分子生物学の進歩により，遺伝性眼疾患の責任遺伝子が同定され，その発症のメカニズムが解明されつつある．それに伴い遺伝性眼疾患に携わる医療従事者に対して，疾患の遺伝形式，再発危険率，遺伝子診断などの遺伝に関するさまざまな情報の提供が求められてきている．さらに，これらの遺伝情報をめぐるさまざまな倫理的問題の対応や心理的・社会的支援も含んだ遺伝カウンセリングの重要性が，今後ますます増していくものと思われる．

Key Words
遺伝カウンセリング
遺伝形式
遺伝性眼疾患
症候群性眼疾患
非症候群性眼疾患

0386-9806/04/¥100/頁/JCLS

はじめに

近年の分子生物学の進歩により，多くの疾患の責任遺伝子が同定されつつある．すでに一部の疾患では，その発症のメカニズムが解明され遺伝子検査による確実な診断が可能になった．それに伴い遺伝性疾患に携わる医療従事者にも，疾患の遺伝形式，再発危険率だけでなく遺伝子診断など遺伝に関するさまざまな情報の提供が求められるようになってきた．またこれらの遺伝情報をめぐるさまざまな倫理的問題も生じてきており，心理的・社会的支援をも含んだ遺伝カウンセリングの必要性が認識されつつある．

眼科疾患についても多くの責任遺伝子が同定され，従来の，視覚電気生理やその他の機能的検査では診断がつかなかった非典型的な眼科疾患も，遺伝子検査による確定診断が可能となった．ヒト遺伝子や遺伝性疾患のカタログであるOMIN（Online Mendelian Inheritance in Man）[1]によると，2004年2月現在，約15,000項目の遺伝子座や疾患が登録されており，そのうち約11,000が遺伝性疾患として分類されている．これらの遺伝性疾患のうち，眼病変を伴うものは約1,400と報告されている．

眼疾患の遺伝について説明する際，眼疾患の存在が単独で存在する非症候群性眼疾患か，あるいは合併症として存在する症候群性眼疾患で

あるか否かで，診断・予後・遺伝形式や再発危険率などがまったく違ったものになってしまう．したがって眼疾患を見た場合には，それ以外の全身性の合併症の存在を必ず念頭におくこと，あるいは疾患のひとつの合併症としての眼疾患の有無を見落とさないことがきわめて重要である．

本稿では，小児科医が日常の臨床の現場で遭遇する可能性が比較的高い，先天的あるいは小児期発症の眼科疾患の遺伝カウンセリングをする際に，留意すべき内容などについて説明する．

遺伝性疾患の分類と再発危険率

遺伝性疾患とは，遺伝子の変異が病因としてかかわる疾患である．それらは大別すると単一の遺伝子の変異が原因でおこる疾患（単一遺伝子病），ミトコンドリアDNAの異常によるミトコンドリア遺伝病，多因子遺伝病，染色体異常からなる．再発危険率とは，ある家系内に一人の患者がいた場合，同じ両親からその次の子が同じ疾患に罹患する確率であり，疾患の遺伝形式や疾患の浸透率によって決まる．遺伝子型の変異により表現型の異常が出現する確率を浸透率という．

1. 常染色体優性遺伝

ヒトの常染色体は，父由来のものと母由来のものがそれぞれ1本ずつ伝わり計2本が存在する．したがって父由来と母由来の同じ遺伝子をそれぞれ一つ，計二つ保有している．その遺伝子のどちらか一方に変異がある場合に発症する遺伝形式を常染色体優性遺伝という．

両親のどちらかが罹患者で遺伝子変異を保有している場合，遺伝子変異が子に伝わり，同じ疾患に罹患する確率は男女を問わず50％となる．浸透率が低い疾患の場合は，両親のどちらかが遺伝子変異を保有していても発症していないこともある．また発症していても症状が軽く，本人に自覚症状がないこともある．その場合は児に遺伝子変異が伝わり，児が明らかな罹患者となってから，親の罹患が判明することもある．

また遺伝子変異を保有していない親から，配偶子の形成期に突然変異により遺伝子変異が生じて，児が罹患者になる突然変異例も認められる．この場合の次子再発危険率はきわめて低い．

2. 常染色体劣性遺伝

常染色体劣性遺伝は，常染色体上に存在する一対二つの遺伝子の両方に変異を有する場合（ホモ接合体）に罹患者となり，一つに遺伝子変異があっても発症せずに保因者となる（ヘテロ接合体）．一般に両親が保因者の場合，子が罹患する確率は25％，子が親と同じ保因者になる確率が50％，まったく遺伝子変異が伝わらない確率が25％という計算になる．

3. X連鎖性劣性遺伝

女性はX染色体が2本存在し，X染色体上の遺伝子を対で保有している．したがって女性の場合，X染色体上の遺伝子の一方に変異があっても，対となっている一方の遺伝子が正常の場合，一般には発症せずに保因者となる．男性はX染色体が1本しか存在しないので，X染色体上の遺伝子に変異があれば罹患者となる．X連鎖性劣性遺伝の場合，保因者の女性と健康な男性との間では，子が遺伝子変異を受け継ぐ確率は男児，女児とも50％である．したがって女児は50％が保因者，50％が正常．男性は50％が罹患者，50％が正常である．

4. ミトコンドリア遺伝

エネルギー産生に関与する細胞質内小器官のミトコンドリアは，核内の遺伝子とは別に独自の遺伝子をもつ．このミトコンドリア遺伝子は，すべて卵子から由来し，母からのみ遺伝する（母系遺伝）．伝えられる変異ミトコンドリアDNAの細胞内，組織内における割合（ヘテロプラスミー）はさまざまであり，そのため遺伝したとしても，発症の程度もさまざまであるため，

再発危険率を正確に評価するのは困難である．

5．多因子遺伝

複数の遺伝子（遺伝要因）と環境要因の相互作用により発症すると考えられる疾患を多因子遺伝病とよぶ．生活習慣病，非症候群性の先天性心疾患や口蓋裂などは多因子遺伝と考えられる．遺伝様式はメンデルの遺伝法則に従わないため，再発危険率は疾患ごとの経験的再発危険率により推定する．

6．染色体異常

染色体異常には数的異常と構造異常がある．一般に数的異常は，配偶子形成の際の不分離という現象によって生じる．この場合，親が同様の数的異常をもつことはほとんどなく，再発危険率はきわめて低い．構造異常の場合は，親が均衡型相互転座を有することがあり，この場合は再発危険率を考慮しなければならない．

眼科疾患の遺伝

1．屈折異常

合併症を伴わない単純屈折異常は，環境要因と遺伝要因が関与する多因子遺伝形式である．

屈折異常を弱度の屈折異常（弱度近視）と，強度の屈折異常（強度近視）に分けると，弱度近視は環境要因の影響が大きく，強度近視は遺伝的要因の影響が大きい．合併症を伴わない強度近視は常染色体優性遺伝形式と考えられ，いくつかの原因遺伝子がすでに報告されている[2)3)]．とくに家系内に屈拙異常の罹患者が多い場合，浸透率が高いと考えられている．実際には他因子の影響も関係しているので屈折異常の再発危険率は4～5%程度と考えられている．

後述するStickler症候群やMarfan症候群などに合併する強度屈折異常は，浸透率がより高い常染色体優性遺伝形式をとる．

2．色覚異常

色覚異常のなかで，多いのは赤や緑の色合いが見分けにくくなる赤緑色覚異常（第一色覚異常と第二色覚異常）であり，これらはX連鎖性劣性遺伝形式をとる．一般の男性の約5%が罹患者で，女性の約10%が保因者である．

平成14年度までは学校健診の一部として色覚検査が行われていたが，平成15年度からは学校保健法の改定により，学校での色覚検査は必ずしも行わなくてもよい項目になった．本人が色覚異常を自覚していなくても日常生活に不便がなければ，色覚異常は，眼疾患というよりは色の見えかたの個性や体質であるともいえることから，家族や本人からの希望がなければ積極的な診断は不要とする考えもある．

一方，色の誤認を自覚できれば日常生活におこる不利益や混乱に対応できること，将来の進路を決める際には，色覚異常には一部の例外的な職業の就業の制限があること，家系内にほかに罹患者がいる場合は，家系内保因者の可能性があることから，自己決定が可能な年齢になった際や，挙児希望の場合には，積極的な診断や詳細な遺伝情報の提供は必要であるとする意見もある．

3．斜　視

ある家系内において斜視の発症が多く認められる事実が報告されており，遺伝性の斜視の存在は古くから指摘されている．

遺伝形式は常染色体優性遺伝，常染色体劣性遺伝，多因子遺伝のいずれも存在すると考えられる[4)]．とくにCongenital general fibrosis syndromeは，浸透率が比較的高い常染色体優性遺伝と考えられている．一般的には多因子遺伝が多いが，両親正常で斜視罹患の児が1人いる場合の再発危険率は約15%程度，両親のいずれかが罹患者の場合は約40%であると見積られている．

4．網膜芽細胞腫

網膜芽細胞種は，以前から小児期発症の遺伝性のがんとして知られており，全体の30%を占

める両眼性網膜芽細胞種はすべて遺伝性である．残りの70％の片眼性網膜芽細胞種のうち10～15％が遺伝性で，全体の55～60％は片眼性で非遺伝性であると考えられる．

常染色体優性遺伝の形式をとるが，浸透率は約90％であり遺伝子変異を受け継いでいても発症しない場合がある．13番染色体長腕14上に位置する癌抑制遺伝子のひとつである*RB*遺伝子が責任遺伝子である[5]．罹患者は二つの*RB*遺伝子に変異を生じている．遺伝性の場合は，配偶子の段階ですでに一つの*RB*遺伝子に変異が存在し，受精後の網膜形成期に，さらに一方の*RB*遺伝子に変異がおこり腫瘍化する．

非遺伝性の場合は，網膜細胞の分化，発達過程で二つの*RB*遺伝子に変異が生じて腫瘍化する（two hit theory）[6]．本症の5～6％の患者に13番染色体長腕14部分の欠失が認められる．この場合は，精神運動発達遅滞や外表奇形を伴う．

5．先天性緑内障

先天性緑内障は，約半数が出生時に約80％が1歳までに発症する．発生頻度は約1/10,000程度で，80％は特発性で20％が遺伝性と考えられる．原発性先天性緑内障は胎生期における前房隅角の形成異常が原因であり，ほかの眼疾患や全身性の合併症は有しないことが多い．常染色体劣性遺伝であるが，再発危険率は10％程度と考えられている．小児期発症の原発開放隅角緑内障の一部は原因遺伝子が同定されており，その場合は，常染色体優性遺伝形式をとる．実際はすべての原因が遺伝によるものではなく，他因子の影響もあるため，再発危険率は5～15％と考えられる．

いずれにしろ家族歴がある場合は，ない場合に比べて明らかに発生頻度が高くなるので，早期からの検査がすすめられる．Stickler症候群，Marfan症候群や無虹彩症などの，ほかの先天異常に合併しておこる続発性先天性緑内障は，これらの疾患の遺伝形式に従う．

6．先天性白内障

先天性白内障の20～30％は遺伝性で，30～50％は特発性である．母体内感染，奇形症候群，代謝異常症，染色体異常なども原因となる．

さまざまな原因遺伝子が報告されており，遺伝形式も常染色体優性遺伝，劣性遺伝形式が報告されている．先天性白内障の多くは常染色体優性遺伝である．とくに両眼性の場合は遺伝性の可能性があるため，児が両眼性の罹患者と診断された場合，家系内に明らかな罹患者がほかにいなくても両親や同胞の検査がすすめられる．

7．無虹彩症

発生頻度は約10万人に1人で，2/3が家族例で1/3は特発例と考えられる．11番染色体短腕13に位置する*PAX6*遺伝子の変異が原因であり[7]，常染色体優性遺伝形式をとる．家系内における無虹彩の表現型はさまざまであり，両側虹彩の完全欠損から虹彩の菲薄化を認めるだけの場合もある．したがって，自覚症状がなくても両親や同胞の眼疾患の有無についての精査が必要である．

無虹彩症の1/3にWilms腫瘍が合併するといわれており，同時に精神発達遅滞や尿道下裂，鼠径ヘルニアなどを合併している場合は，WAGR（Wilms tumor, aniridia, genitourinary abnormalies, mental retardation）症候群とよばれる[8]．この場合，多くの症例で11番染色体短腕13の欠失が認められ，*PAX6*遺伝子と近傍に位置する*WT1*遺伝子の欠失が原因である．したがって無虹彩症が認められた場合には，染色体検査（FISH法）を行い，11番染色体短腕13部分の欠失や，この部分を切断点とする染色体構造異常の有無を確認することが重要である．

8．レーベル視神経萎縮症

10歳代から20歳代にかけて，急性または亜急性の両眼性視力低下で発症する．患者の80％は男性患者である．ミトコンドリアDNAに点

突然変異がみられ，日本人の罹患者の約90％に共通の変異が認められる．しかし，遺伝子変異をもっていても男性では約40％，女性では約20％しか発症せず，また女性を介して遺伝するため，父親が罹患者の場合は遺伝しない．

再発危険率は，経験的再発危険率により母親が罹患者あるいは母親に症状はないが，前児が罹患者の場合，次子が男児の場合は約50％，女児の場合は約20％が罹患者となる．女児の約80％は保因者となる．小児期早期に発症する視神経萎縮症でレーベル視神経萎縮症と鑑別を要する疾患に，常染色体優性視神経萎縮があるが，本症は常染色体優性遺伝形式をとる．

9．症候群性眼疾患

眼疾患に加えて広範な合併症を伴う場合は，眼疾患を伴う症候群として診断され，単独の眼疾患とは違った遺伝形式や病態をとることがある．小児科診療で比較的受診する機会が多いと思われる眼疾患を伴う症候群について，遺伝性疾患について説明する．

1）Stickler症候群

強度の近視と小下顎，口蓋裂が特徴である．その他には関節症状や眼球の軽度突出などの特異顔貌，僧房弁逸脱，聴力障害などを伴うこともある．12番染色体上にマップされる*COL2A1*遺伝子が責任遺伝子である[9]．常染色体優性遺伝であるが，表現型には差があり，必ずしも家系内の罹患者は同様の症状をとるわけではない．児に口蓋裂，小下顎症による呼吸困難などのPierre Robin Sequenceを認めた場合には，屈折異常，白内障や網膜剥離など眼病変の有無を検査することをすすめる．また親にいずれかの症状があった場合は，よりいっそうStickler症候群の可能性を考える．

2）Marfan症候群

高身長，側彎・後彎など骨格異常，僧房弁逸脱・大動脈基部の拡張などの循環器病変，眼症状を伴う．眼症状は多くに近視を認め，50～80％に片側あるいは両側の水晶体変位を認める．染色体優性遺伝で浸透率は高いが，表現型には差があるため家系内の病歴や体型にも注意をはらう．

3）Goldenhar症候群（鰓弓症候群，眼・耳介・椎骨症候群）

同側の眼球類皮腫（デルモイド），片側の耳介変形（無耳，外耳道閉鎖から副耳のみまでさまざま），顔面の非対称などを呈し，一部の罹患者は椎骨の変形を伴う．頻度は5,000～25,000人に1人である．軽症例から重症例までさまざまであり，診断基準によって診断が左右される．ほとんどが特発例で多因子遺伝が考えられるが，まれに常染色体優性遺伝，常染色体劣性遺伝やX連鎖劣性遺伝を示す家系が存在する．特発例の場合，経験的再発危険率は2～3％である．

4）Lowe症候群（Oculo-cerebrorenal syndrome of Lowe）

両側の先天性白内障がほぼ必発し，その他，緑内障・角膜変性などの眼症状，新生児期の筋緊張低下，精神発達遅滞および腎尿細管性アシドーシスを呈する．X連鎖性劣性遺伝形式をとるが，まれに女児であっても症状を呈することがあるので注意を要する[10]．保因者の95％に眼病変が存在するため，眼病変有無は保因者診断に有用である．母親の眼病変を認めた場合は，次子再発危険率の情報提供が可能である．

5）ガラストース血症

ガラストース分解酵素の欠損などによる代謝異常のため，ガラストースや中間代謝産物が蓄積することで，白内障に加えて，嘔吐・下痢などの消化器症状や肝機能障害を呈する．新生児マス・スクリーニングの対象となっており，早期に発見されれば予後はよい．欠損酵素によりⅠ～Ⅲ型に分類されているが，いずれも責任遺伝子は同定されており，常染色体劣性遺伝形式をとるため再発危険率は25％である．

おわりに

遺伝性疾患の児をもった親は，多かれ少なかれ自責の念をもっており，また次子への再発を憂慮している．患者や家族から遺伝相談を求められた場合，単に遺伝形式や再発危険率などの遺伝情報を告げるだけではなく，これらの情報をもとに，患者や家族が遺伝にかかわる問題について，正しい自己決定ができるように援助することが必要である．

また，遺伝性疾患の遺伝子検査においては，検査目的とその結果の及ぼす影響について，医療者側も患者側もよく理解したうえで行うべきである．患者の確定診断や予後を推測するために行うのか，遺伝子検査の結果を用いて家系内での保因者診断，および出生前診断の応用まで念頭において行うのか，など検査の目的を明確にしておくべきである．そして検査の実施が，技術的・倫理的に可能であるのかについても，あらかじめよく検討すべきである．また必要に応じて適切な遺伝カウンセリングが受けられるように，施設の情報を提供しておくことも重要である．

●文　献

1) http://www.ncbi.nlm.nih.gov/entrez/query.fcgi?db=OMIM&tool=toolbar
2) Young TL, Ronan SM, Alvear AB et al.: A second locus for familial high myopia maps to chromosome 12q. Am J Hum Genet 63: 1419-1424, 1998
3) Young TL, Ronan SM, Alvear AB et al.: A genome wide scan for familial high myopia suggests a novel locus on chromosome 7q36. J Med Genet 39: 118-124, 2002
4) O'hara MA, Nelson LB: Heredity of strabismus 59. Biochemical foundation of ophthalmology, volume 3. Harper and Row, Philadelphia, 1993
5) Friend SH, Bernards R, Rogelj S et al.: A human DNA segment with properties of the gene that predisposes to retinoblastoma and osteosarcoma. Nature 323: 643-646, 1986
6) Knudson AG Jr: Mutation and cancer: statistical study of retinoblastoma. Proc Natl Acad Sci USA 68: 820-823, 1971
7) Hanson IM, Seawright A, Hardman K et al.: PAX6 mutations in aniridia. Hum Mol Genet 2: 915-920, 1993
8) Riccardi VM, Sujansky E, Smith AC: Chromosomal imbalance in the Aniridia-Wilms'tumor association: 11p interstitial deletion. Pediatrics 61: 604-610, 1978
9) Ahmad NN, Ala-Kokko L, Knowlton RG et al.: Stop codon in the procollagen II gene (*COL2A1*) in a family with the Stickler syndrome (arthro-ophthalmopathy). Proc Natl Acad Sci USA 88: 6624-6627, 1991
10) Hodgson SV, Heckmatt JZ, Hughes E et al.: A balanced de novo X/autosome translocation in a girl with manifestations of Lowe syndrome. Am J Med Genet 23: 837-847, 1986

著者連絡先

〒157-8535　東京都世田谷区大蔵2-10-1
国立成育医療センター遺伝診療科
小須賀基通

ARTICLE

doi:10.1016/S1525-0016(03)00262-4

Improvement of Skeletal Lesions in Mice with Mucopolysaccharidosis Type VII by Neonatal Adenoviral Gene Transfer

Arihiko Kanaji,[1,2,3] Motomichi Kosuga,[1,3,4] Xiao-Kang Li,[1] Yasuyuki Fukuhara,[1,3,4] Akiko Tanabe,[1] Yuko Kamata,[1,3] Noriyuki Azuma,[1,3] Masao Yamada,[1] Toyonori Sakamaki,[2,3] Yoshiaki Toyama,[2] and Torayuki Okuyama[1,3,4,*]

[1]*National Research Institute of Child Health and Development, Tokyo 157-8535, Japan*
[2]*Department of Orthopedics and* [4]*Department of Pediatrics, Keio University School of Medicine, Tokyo 160-8582, Japan*
[3]*National Center for Child Health and Development, Tokyo 157-8535, Japan*

**To whom correspondence and reprint requests should be addressed at the Department of Clinical Genetics and Molecular Medicine, National Center for Child Health and Development, 2-10-1 Okura Setagaya-ku, Tokyo 157-8535, Japan. Fax: +81-3-3416-2222. E-mail: okuyama-t@ncchd.go.jp.*

Neonatal gene transfer using adenovirus vectors expressing human β-glucuronidase (AxCAhGUS) resulted in pathological improvement in multiple visceral organs of mice with mucopolysaccharidosis type VII (MPSVII). However, the therapeutic effect on skeletal deformities and growth retardation, the major clinical symptoms in MPSVII, was not fully investigated by biochemical and histopathological analyses. In this study, we injected AxCAhGUS into a murine model of MPSVII (B6/MPSVII) within 24 h of birth and evaluated the therapeutic effects on skeletal deformities and growth retardation. High levels of β-glucuronidase (GUSB) activity (approximately threefold higher than normal GUSB activity) were observed in the articular cartilage of the mice 30 days after the treatment. Histopathological study in the knee joints showed elimination of vacuole cells in the articular cartilage and growth plate. Subchondral bone near the articular surface was almost normal in the treated MPSVII mice. Long-term observation (for 140 days after treatment) indicated that characteristic phenotypes such as flattened face, hunched stature, and shortening of bone length in the treated mice were almost normal. These results demonstrate that a single injection of adenovirus vector into neonatal MPSVII mice is sufficient for long-term normalization of skeletal deformities and effective in pathological correction of the articular cartilage and growth plate.

Key Words: mucopolysaccharidosis, adenovirus, skeletal lesions, gene therapy

INTRODUCTION

Mucopolysaccharidosis type VII (MPSVII, Sly disease)is a lysosomal storage disease caused by a deficiency of β-glucuronidase (GUSB) activity, which results in a progressive accumulation of undegraded glycosaminoglycans in the lysosomes [1]. MPSVII is characterized pathologically by lysosomal distension in many tissues and clinically by hepatosplenomegaly, mental and growth retardation, hearing and vision defects, skeletal deformities, and short life span [2].

B6/MPSVII is a murine model of MPSVII, sharing characteristic phenotypes and pathological abnormalities with human MPSVII [3–5]. In this model, a single base pair deletion in exon 10 of the GUSB gene results in the formation of a premature stop codon, leading to the complete absence of GUSB activity [3].

B6/MPSVII is a useful model to develop novel therapeutic approaches, such as enzyme replacement therapy (ERT) and bone marrow transplantation (BMT) [6–12]. In adult MPSVII mice, ERT and BMT will reverse visceral lesions and prolong survival, but have little effect on growth retardation, bone dysplasia, or lysosomal storage in the central nervous system [6,7]. In contrast, neonatal MPSVII mice receiving ERT or BMT showed an improvement in skeletal deformities [7,11,12]. Sands *et al.* reported on the therapeutic effect of BMT on skeletal deformities during the neonatal period [11]. They showed pathological improvement of the articular surface, growth

1525-0016/03 $30.00

plate, and cortical bone in the treated MPSVII mice. Voglar *et al.* reported on the therapeutic effect of ERT on skeletal deformities during the neonatal period [12]. In their study, recombinant β-glucuronidase enzyme was administered intravenously into MPSVII mice at weekly intervals from birth to 6 weeks of age. Slight elimination of vacuolated osteocytes and osteoblasts was shown in the treated mice 14 days after the last injection of ERT. However, both BMT and ERT have limitations for the treatment of human MPSVII. For BMT, a shortage of suitable donors makes it difficult to apply widely. ERT requires frequent injections of the purified enzymes, which is very expensive in general. For these reasons, another treatment strategy has to be developed to improve skeletal deformities in MPSVII.

Recently, gene therapy for MPSVII including *in vivo* and *ex vivo* gene transduction approaches has been attempted using several viral vectors such as retroviruses [13–19], herpesviruses [20,21], adenoviruses [22–29], lentiviruses [30,31], and adeno-associated viruses [32–35]. Several types of cells, such as bone marrow cells [16], fibroblasts [17], and myoblasts [18], were transduced with retroviral vectors, and the cells overexpressing GUSB were administered into adult MPSVII mice locally as well as systemically. Limited correction of lysosomal storage in the liver and spleen was demonstrated following these *ex vivo* gene therapies. An *in vivo* gene therapy approach has also been successful for generating tissues overexpressing GUSB. We administered an E1/E3-deleted adenoviral vector expressing GUSB (AxCAhGUS) into MPSVII mice via the tail vein and demonstrated that high levels of GUSB were observed in the liver, spleen, kidney, lung, and heart [27].

We previously reported that intravenous administration of AxCAhGUS during the neonatal period was sufficient to improve facial and cranial bone deformities in mice with MPSVII [29]. Ponder *et al.* described remarkable improvement of skeletal-articular lesions in dogs with MPSVII after retroviral gene transfer shortly after birth [19]. Daly *et al.* also reported that AAV-mediated gene transfer during the neonatal period resulted in a remarkable improvement of characteristic phenotypes, such as flattered face, hunched stature, and shortening of bone length [35]. However, the therapeutic effect on skeletal deformities and growth retardation, the major symptoms in MPSVII, was not fully investigated by biochemical and histopathological analysis in these papers.

Here, we administered AxCAhGUS intravenously and evaluated the therapeutic effects on skeletal deformities and growth retardation in mice with MPSVII. These analyses demonstrate that the improvement of growth disturbance and pathological correction of the articular cartilage and growth plate are achievable by a single adenoviral administration into neonatal MPSVII mice.

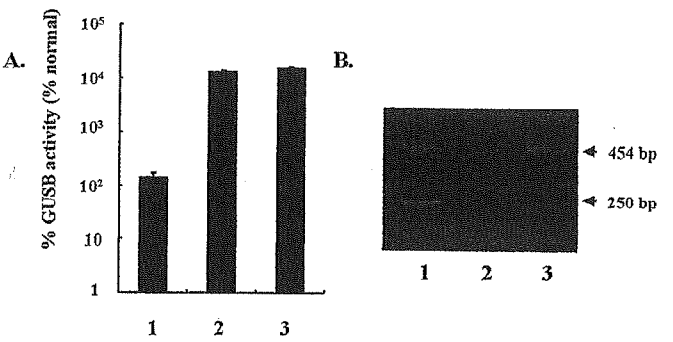

FIG. 1. Therapeutic efficacy in the articular cartilage of B6/MPSVII mice infected with AxCAhGUS in adulthood. (A) We injected 1.0 ml of viral solution containing 1×10^8 pfu of AxCAhGUS into adult B6/MPSVII mice (12–15 weeks of age). The mice were sacrificed 7 days after intravenous administration. The GUSB activities in the articular cartilage (lane 1), liver (lane 2), and serum (lane 3) were measured. Results are expressed as the percentage of GUSB activity found in the corresponding organs from four age-matched B6 (+/+) mice. (B) DNA from the articular cartilage and liver was extracted and used as templates for PCR. Virally encoded human GUSB cDNA in AxCAhGUS produced a 240-bp band, and the murine GUSB gene produced a 454-bp band. Both 454- and 240-bp DNA fragments were amplified when PCR was performed using DNA from the liver as templates, while a single 454-band was amplified by PCR using DNA from the articular cartilage as templates. In each group, four mice were used, and representative results are shown (lane 1, liver; lane 2, articular cartilage; lane 3, articular cartilage).

RESULTS

Therapeutic Effect on Articular Cartilage of the MPSVII Mice Treated in Adulthood

To evaluate the therapeutic efficacy of adenovirus-mediated gene therapy on articular cartilage of MPSVII mice, we sacrificed the gene-transduced adult B6/MPSVII mice 7 days after intravenous administration of 1×10^8 plaque-forming units (pfu) of AxCAhGUS. We determined GUSB activity using 4-methylumbelliferyl β-D-glucuronide as substrate. We observed high levels of GUSB activity (1.5-fold higher than normal GUSB activity) in the articular cartilage (Fig. 1A, lane 1). In the liver, high levels of GUSB activity were also detected (Fig. 1A, lane 2). Moreover, to determine whether the origin of GUSB activity in the articular cartilage was due to transgene expression or due to cross-correction of lysosomal GUSB, we performed a PCR-based assay to detect virally encoded DNA in the articular cartilage. The PCR primers were designed based on the sequences of exon 6 and exon 7 of the human GUSB gene to amplify a 240-bp fragment from the human GUSB cDNA in the viral genome of AxCAhGUS. This PCR also generates a 454-bp fragment from the endogenous murine GUSB gene [27]. The 454-bp DNA fragment corresponding to the partial endogenous murine GUSB gene was amplified; however, the 240-bp partial human GUSB cDNA located in AxCAhGUS was not amplified (Fig. 1B) from the DNA of the articular cartilage, suggesting that GUSB detected in the articular cartilage was the result of

doi:10.1016/S1525-0016(03)00262-4

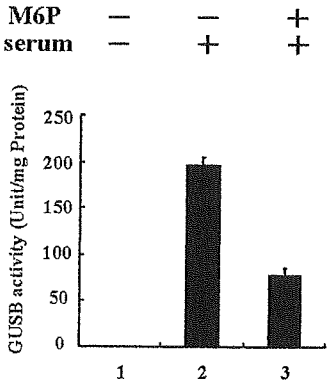

FIG. 2. Mannose 6-phosphate receptor-mediated endocytosis of GUSB in mouse chondrocytes. The articular cartilage from untreated MPSVII mice was incubated with medium with the serum from MPSVII mouse injected with 1×10^8 pfu of AxCAhGUS 7 days before. The serum contained 3.1×10^3 units of GUSB. The GUSB activity in the articular cartilage incubated with the serum was dramatically increased (lane 2); however, the increase was significantly suppressed when the articular cartilage was incubated in the presence of 6 mM mannose 6-phosphate (lane 3). The endogenous GUSB activity in the articular cartilage of MPSVII mice was negligible (lane 1).

in vivo cross-correction rather than direct gene transduction.

GUSB Cross-correction Mediated by the Mannose 6-phosphate Receptors in Chondrocytes

Cross-correction of many lysosomal enzymes is mediated mainly by the mannose 6-phosphate receptors expressed on cell surface membranes, and this process is efficiently blocked by mannose 6-phosphate [27]. To confirm that cross-correction mediated by mannose 6-phosphate receptors contributed to the high levels of GUSB activity in the articular cartilage of the treated MPSVII mice, we cocultured articular cartilage of the untreated MPSVII mice with medium containing serum obtained from the gene-transferred MPSVII mice. The GUSB activity was dramatically increased in the articular cartilage cocultured with serum containing 3.1×10^3 units of GUSB (Fig. 2, lane 2). Furthermore, the increase in GUSB activity was significantly reduced when 6 mM mannose 6-phosphate was present in the medium (Fig. 2, lane 3). These observations suggest that the GUSB enzyme was taken up by articular chondrocytes via the mannose 6-phosphate receptors.

Therapeutic Effects on Skeletal Deformities and Growth Retardation after Administration of AxCAhGUS during the Neonatal Period

Intravenous administration of AxCAhGUS in adulthood has little effect on growth retardation and skeletal deformities in MPSVII mice, because skeletal deformities and growth retardation are progressive from the neonatal period in mucopolysaccharidoses. To prevent skeletal deformities and growth retardation from progressing in MPSVII mice, we started treatment during the neonatal period. We injected 1×10^7 pfu of AxCAhGUS via the superficial temporal vein into the newborn MPSVII mice within 24 h of delivery and evaluated the therapeutic effect on skeletal deformities and growth retardation. Long-term observation (140 days after the treatment) demonstrated a remarkable improvement of growth retardation in the mice treated during the neonatal period (Fig. 3A2). The lengths of the tibia and fibula of the treated MPSVII mice were almost indistinguishable from those of their normal littermates (Fig. 3B2). These results demonstrate that morphological normalization of skeletal deformities in MPSVII is apparently achievable when the treatment starts during the neonatal period.

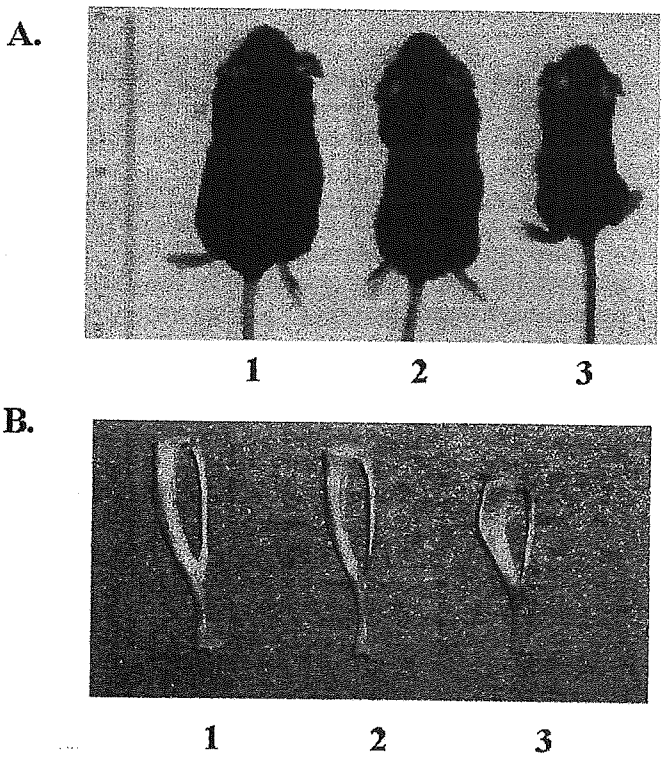

FIG. 3. Therapeutic effect on skeletal deformities and growth retardation in neonatally treated mice with MPSVII. (A) Growth retardation is a characteristic symptom of mice with B6/MPSVII. We injected 100 μl of viral solution containing 1×10^7 pfu of AxCAhGUS via the superficial temporal vein into neonatal B6/MPSVII mice within 24 h of delivery and evaluated the therapeutic effect on skeletal deformities and growth retardation 140 days after the treatment. The body length of the treated MPSVII mice (2) was indistinguishable from that of a B6 (+/+) littermate (1), while an untreated MPSVII littermate looked remarkably short (3). (B) The shape and length of the tibia and fibula of the neonatally treated mice (2) were compared with those of their affected (3) or normal (1) littermates. The long bones of the MPSVII mice (3) were significantly short and wide compared with those of their normal littermates (1), and the long bones of the treated MPSVII mice (2) show length and shape similar to those of their normal littermates.

Biochemical Analysis of Articular Cartilage in the Mice Treated during the Neonatal Period

To evaluate the therapeutic effect on skeletal deformities in more detail, we performed biochemical analysis. We sacrificed MPSVII mice treated during the neonatal period 30 days after the treatment and measured GUSB activities in the articular cartilage and liver (Figs. 4A and 4B). We observed high levels of GUSB activity (631.9 ± 69.9 unit/mg protein) corresponding to more than threefold higher than normal GUSB activity in the articular cartilage of the treated mice (Fig. 4A, lanes 1 and 2). In the liver, high levels of GUSB activity were also detected (Fig. 4A, lanes 3 and 4). We isolated chondrocytes from the articular cartilage of MPSVII mice and performed GUSB activity staining on the chondrocyte culture. About 40% of the chondrocytes from the MPSVII mice treated with AxCAhGUS were GUSB-positive cells (Fig. 4B). PCRs demonstrated that viral DNA was detectable in the articular cartilage of the MPSVII mice treated during the neonatal period (Fig. 4C). These results suggested that the articular cartilage was efficiently transduced with an adenoviral vector and extremely high levels of transgene expression could be obtained, when the mice were treated during the neonatal period.

Histopathological Analysis of Skeletal Lesions in the Mice Treated during the Neonatal Period

We compared histopathological analysis in the knee joint after the neonatal treatment (Figs. 5B, 5E, and 5H) with age-matched normal (Figs. 5A, 5D, and 5G) and untreated MPSVII mice (Figs. 5C, 5F, and 5I). Extensive vacuolization of the cells in the articular cartilage was not completely eliminated; however, they were obviously reduced in size and number after the treatment (Fig. 5B). The normal columnar architecture in the growth plate (resting zone, proliferative zone, hypertrophic zone, and endochondral; bone) was completely disrupted in the untreated MPSVII mice (Fig. 5F); however, we observed columnar architecture in the proliferative and hypertrophic zones in the MPSVII mice treated with neonatal gene therapy (Fig. 5E). Subchondral bone and bone marrow cells near the articular surface were significantly improved in the treated MPSVII mice (Fig. 5H). These results demonstrate that limited but significant improvement of pathological lesions in bone tissues was achieved in the gene-transduced MPSVII mice.

Discussion

Skeletal deformities and growth retardation are frequent manifestations of mucopolysaccharidoses. Multiple skeletal abnormalities, including short stature, angular deformities of the ribs, abnormally short forelimbs, subluxation of the hip joints, and epiphyseal dysplasia involving the vertebrae and long bones were observed in feline and murine models of MPSVII [4,36].

The pathogenesis of skeletal deformities and growth retardation was studied using several models of mucopolysaccharidoses [37,38]. Abreu *et al.* reported that clusters of distended chondrocytes disrupted the normal columnar architecture of the growth plate, presumably leading to bone growth abnormalities [37]. Simonaro *et al.* demonstrated that accumulated dermatan sulfate in the chondrocytes enhanced apoptosis of the articular cartilage cells in MPSVI cats, leading to degeneration of the articular surface [38]. These results suggest that abnormal chondrocytes in the articular cartilage and growth plate play an important role in skeletal deformities and growth retardation in mucopolysaccharidoses.

Recently, several reports have demonstrated that neonatal gene therapy contributed to a remarkable improvement of skeletal deformities in MPSVII mice [19,29,35]. However, histopathological and biochemical analyses of the skeletal lesions were not performed in these reports. Here, we demonstrated improvements in skeletal architecture and bone pathology in MPSVII mice by adenovirus-mediated gene therapy during the neonatal period.

Histopathological abnormality of the growth plate has been well characterized in other types of mucopolysaccharidoses [37,39]. Abreu *et al.* reported that poorly organized proliferative and hypertrophic zones were observed in the growth plate of MPSVI cats [37]. Silvery *et al.* also reported that the normal columnar architecture of the proliferative and hypertrophic zones was disrupted in the growth plate of a human patient with Hurler's syndrome [39]. In this study, almost total loss of the proliferative and hypertrophic zones was shown in the growth plate of untreated MPSVII mice, while a columnar architecture of the proliferative and hypertrophic zones was demonstrated in the growth plate of MPSVII mice following neonatal gene therapy. These results suggest that pathological improvement of the proliferating and hypertrophic zones in the growth plate is important for the normalization of growth retardation and bone development in MPSVII mice treated by neonatal gene transfer.

Moreover, biochemical analysis of the articular cartilage was performed following adult and neonatal gene therapy. When we injected adenoviral vectors into adult MPSVII mice, most of the vectors were distributed predominantly in the liver [27]. The GUSB enzyme was secreted mainly from hepatic cells and significantly taken up by other cells via the mannose 6-phosphate receptors expressed on the cell surface membrane. This pathway is called *in vivo* cross-correction. Our results demonstrated that this *in vivo* cross-correction mechanism also contributed to high levels of GUSB activity in the articular cartilage of the treated MPSVII mice following adult gene therapy. On the other hand, we previously reported that adenoviral vectors were distributed in multiple organs such as the liver, lung, heart, spleen, kidney, and brain in MPSVII mice treated by neonatal gene therapy [29]. In this study, a PCR-based method demonstrated that viral

doi:10.1016/S1525-0016(03)00262-4

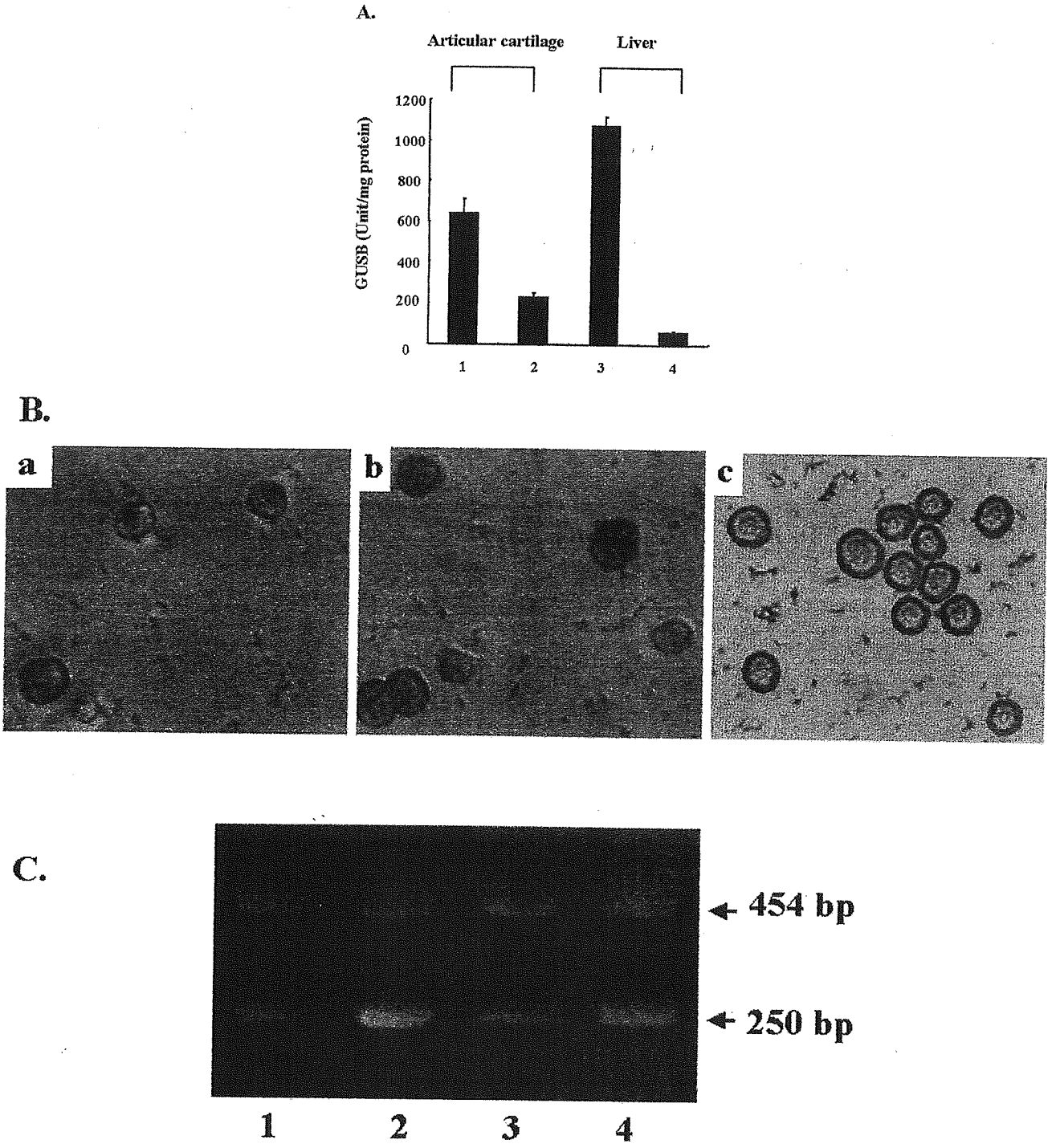

FIG. 4. Biochemical analysis of the articular cartilage of B6/MPSVII mice infected with AxCAhGUS in the neonatal period. (A) The mice treated during the neonatal period were sacrificed 30 days after the treatment and the GUSB activity in the articular cartilage and liver was measured. High levels of GUSB activity were observed in the articular cartilage (lane 1) and liver (lane 3) of the treated mice. (Lane 1, articular cartilage from the treated mice; lane 2, articular cartilage from normal B6 mice; lane 3, liver from the treated mice; lane 4, liver from normal B6 mice.) (B) Biochemical analysis with naphthol AS-BI β-*d*-glucuronide was also performed. Only GUSB-positive cells were observed in cells of B6 (+/+) mice (a). GUSB-positive chondrocytes (stained red) were identified in the treated MPSVII mice (b), while no GUSB-positive cells were observed in untreated MPSVII mice (c). (C) DNA from chondrocytes and livers was extracted and used as templates for PCR. Virally encoded human GUSB cDNA in AxCAhGUS generated a 240-bp band, and the murine GUSB gene produced a 454-bp band. Both the 240- and the 454-bp DNA fragments were amplified in both the articular cartilage and the liver. In each group, two mice were used for this experiment, and representative results are shown (lanes 1 and 2, liver; lane 3, articular cartilage; lane 4, articular cartilage).

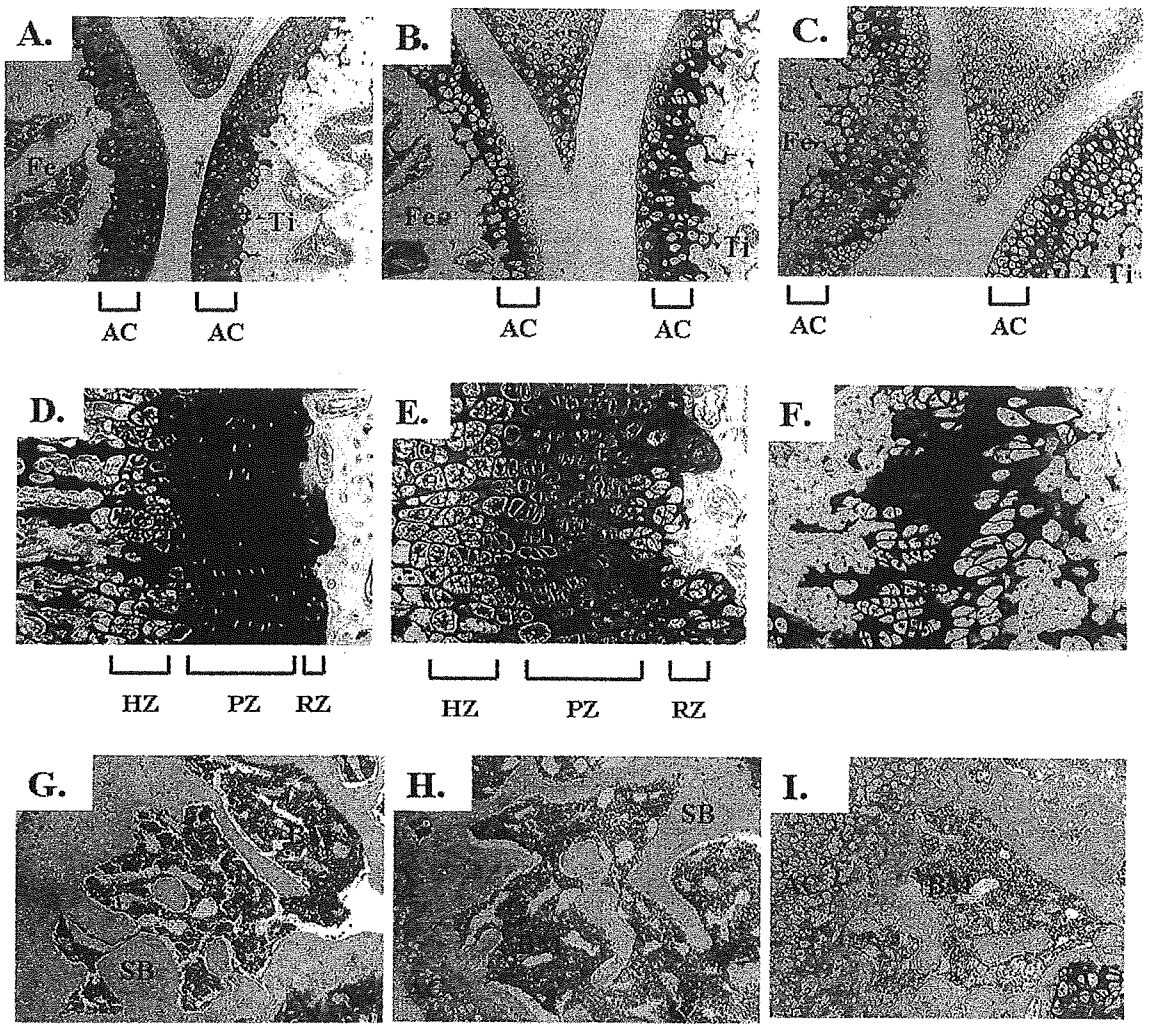

FIG. 5. Histopathological analysis of the epiphysis and metaphysis of the knee joint of B6/MPSVII mice treated with AxCAhGUS during the neonatal period. The mice that received adenoviral vectors during the neonatal period were sacrificed 30 days after the treatment, and pathological improvement in the articular cartilage and growth plate of the knee joint was evaluated. Toluidine blue staining of the epiphysis of normal mice (A), MPSVII mice 30 days after the treatment (B), and untreated MPSVII mice (C) is shown. Original magnification ×10. Moderate elimination of vacuole cells in the articular cartilage was observed in the treated mice with MPSVII. Toluidine blue staining of the metaphysis of normal mice (D), MPSVII mice 30 days after the treatment (E), and untreated MPSVII mice (F) is shown. Original magnification ×20. Moderate elimination of vacuole cells in the growth plate was also observed in the treated mice with MPSVII. Hematoxylin–eosin staining of the subchondral bone of normal mice (G), MPSVII mice 30 days after the treatment (H), and untreated MPSVII mice (I) is shown. Original magnification ×20. The subchondral bone near the articular surface was almost normal in the treated MPSVII mice. AC, articular cartilage; Fe, femur; Ti, tibia; GP, growth plate; RZ, resting zone; PZ, proliferative zone; HZ, hypertrophic zone; SB, subchondral bone; BM, bone marrow.

DNA was also detected in the articular cartilage after neonatal gene transfer. This result means that high levels of GUSB activity detected in the articular cartilage are not only due to *in vivo* cross-correction, but also due to transgene expression following neonatal gene therapy.

Successful *in vivo* gene transduction into murine articular chondrocytes during the neonatal period is the most important finding in this study. Gene transduction into the articular tissues has been already reported [40–42]. Arai *et al.* demonstrated *ex vivo* gene transduction into murine articular chondrocytes using adenoviral vectors [40]. In their study, efficient transgene expression was observed in the chondrocytes for at least 21 days. However, *in vivo* gene transduction into the articular chondrocytes was not successful when an intra-articular injection of viral vectors was carried out in adulthood [41,42].

There is a significant difference in the characterization of articular cartilage between adult and neonatal mice. The articular cartilage consists of sparse chondrocytes and a dense extracellular matrix. Each chondrocyte in the articular cartilage is isolated to its own lacuna and is surrounded by the extracellular matrix. The articular car-

doi:10.1016/S1525-0016(03)00262-4

tilage in adulthood is an avascular area and is nourished by synovial fluid diffusion. However, the articular cartilage during the neonatal period is adequately supplied with epiphyseal vessels [43]. When an intravenous administration of AxCAhGUS was given to neonatal MPSVII mice, the vector could transduce the articular chondrocytes via the artery.

To prevent the progression of skeletal deformity and growth retardation in MPSVII mice, persistent high levels of GUSB activity in the skeletal lesion should be maintained for at least 4 weeks after neonatal treatment, because the growth period of these mice is usually from birth to 4–8 weeks of age. In this paper, high levels of GUSB activity were observed in the articular cartilage 30 days after neonatal gene transfer. Moreover, we previously demonstrated the time-dependent change of serum GUSB activity in mice infected with AxCAhGUS during the neonatal period [29]. In that report, high levels of GUSB activity (10-fold higher than normal GUSB activity) were also observed in sera from treated mice 5 weeks after neonatal administration of AxCAhGUS. These results suggest that the persistent high levels of GUSB activity in MPSVII mice during the neonatal period are sufficient for not only histopathological improvement of articular cartilage and growth plate, but also remarkable improvement of growth retardation in MPSVII mice following neonatal gene therapy.

Here, we demonstrated the therapeutic effect on skeletal abnormalities using a murine model of MPSVII. It is important to prevent skeletal deformities from progressing in mucopolysaccharidoses and neonatal treatment is desirable for this purpose. Although several safety issues have to be resolved before clinical application, this neonatal gene therapy using an adenoviral vector is a promising strategy for treating the skeletal deformities of MPS-VII and other lysosomal storage diseases.

Materials and Methods

Generation of a recombinant adenovirus expressing human GUSB. An adenovirus, AxCAhGUS, for human GUSB was constructed by the COS-TPC method described previously [27]. A cosmid, AxCAhGUS, which contained an expression cassette of human GUSB under the control of the CAG promoter, was constructed by subcloning cDNA for human GUSB at a unique *SwaI* site of pAxCAwt. 293 cells were cotransfected with cosmid pAxCAhGUS and the adenovirus DNA–terminal protein complex, which had already been digested at several sites with *Eco*T22I. A recombinant adenovirus was generated through homologous recombination in the 293 cells.

Animals. Syngeneic B6 (+/+) and B6/MPSVII (mps/mps) mice were obtained from a pedigree colony of B6.C-H-2^{bml}/ByBir-gus^{mps}/+ maintained at the National Research Institute of Child Health and Development. All mice were maintained in accordance with the guidelines of the animal committee of the facility.

Quantitative analysis of GUSB in the articular cartilage and liver. The articular cartilage was removed from the bilateral patella, femoral head, and humeral head. The articular cartilage and liver were washed in Dulbecco's modified Eagle's medium (DMEM; Nissui Pharmaceutical, Tokyo, Japan). GUSB activities were measured in tissue homogenates using a fluorometric assay described previously [44]. Briefly, pellets were homogenized in 10 mM Tris–HCl (pH 7.5), 150 mM NaCl, 0.2% Triton X-100, and 1 mM dithiothreitol and centrifuged at 14,000 rpm for 1min to remove debris. The GUSB activities were measured using 4-methylumbelliferyl β-*d*-glucuronide (Sigma, St. Louis, MO) as substrate.

Isolation of chondrocytes from the articular cartilage and GUSB activity staining of the articular chondrocytes. Chondrocytes were isolated as previously described [40]. The articular cartilage was cut into pieces in DMEM supplemented with 10% fetal bone serum (FBS; Gibco BRL, Gaithersburg, MD), and treated with 0.025% collagenase and incubated at 37°C until the fragment was digested. Residual multicellular aggregates were removed by centrifugation, and cells were washed three times in DMEM, 5% FBS before the experiments. The chondrocytes were incubated in 24-well plates with a total volume of 1 ml of DMEM supplemented with 10% FBS for 2 days. GUSB activity staining was performed on the chondrocyte culture using naphthol AS-BI β-*d*-glucuronide (Sigma) as substrate, as previously described [27].

Detection of viral DNA in the articular cartilage. Total DNA of the tissue samples was extracted using a QIAamp DNA mini kit (Qiagen GmbH, Hilden, Germany) according to the manufacturer's protocol. Viral DNA of AxCAhGUS was detected using PCR to amplify the partial cDNA for human GUSB. The forward and reverse primers were synthesized based on the sequences of exon 6 (5′-CTGTGGCTGTCACCAAGAGC-3′) and exon 7 (5′-GGACACTCATCGATGACCAC-3′) of human GUSB cDNA. The sequences were identical to those of human cDNA, but had two mismatches within the murine exon 6 sequence. One hundred microliters of the PCR mixture contained 250 μM dNTPs, 10 pmol of the forward and reverse primers, 1 μg of purified DNA, and 2.5 U of *Taq* DNA polymerase (TaKaRa). Thirty cycles of PCR were carried out at 94°C for 90 s, 56°C for 90 s, and 72°C for 90 s. The expected products were a 240-bp fragment from cDNA and a 454-bp fragment from the endogenous murine gene.

Histopathology of the knee joints. Mice were sacrificed by cervical dislocation. Thereafter, the knee joints were removed and fixed in 10% formalin. After decalcification in 5% formic acid, the specimens were embedded in paraffin, sectioned at 5 μm, and stained with toluidine blue and hematoxylin–eosin. Histopathological sections were evaluated morphologically by light microscopy [40].

Acknowledgments

We thank Drs. Y. Kanegae and I. Saito for recombinant adenovirus constructs and Dr. J. Miyazaki for the CAG promoters. This work was supported in part by grants for Pediatric Research from the Ministry of Health, Labor, and Welfare, Japan, and by grants for Research on Health Sciences Focusing on Drug Innovation from the Japan Health Sciences Foundation.

RECEIVED FOR PUBLICATION MAY 27, 2003; ACCEPTED JULY 28, 2003.

References

1. Sly, W. S., Quinton, B. A., McAlister, W. H., and Rimoin, D. L. (1973). β-Glucuronidase deficiency: report of clinical, radiologic, and biochemical features of a new mucopolysaccharidosis. *J. Pediatr.* **82:** 249–257.
2. Birkenmeier, E. H., *et al.* (1989). Murine mucopolysaccharidosis type VII: characterization of a mouse with beta-glucuronidase deficiency. *J. Clin. Invest.* **83:** 1258–1266.
3. Sands, M. S., and Birkenmeier, E. H. (1993). A single-base-pair deletion in the beta-glucuronidase gene accounts for the phenotype of murine mucopolysaccharidosis type VII: a single-base-pair deletion in the beta-glucuronidase gene accounts for the phenotype of murine mucopolysaccharidosis type VII. *Proc. Natl. Acad. Sci. USA* **90:** 6567–6571.
4. Vogler, C., *et al.* (1990). A murine model of mucopolysaccharidosis VII: gross and microscopic findings in beta-glucuronidase-deficient mice. *Am. J. Pathol.* **136:** 207–217.
5. Sands, M. S., *et al.* (1997). Gene therapy for murine mucopolysaccharidosis type VII. *Neuromuscul. Disord.* **7:** 352–360.
6. Birkenmeier, E. H., *et al.* (1991). Increased life span and correction of metabolic defects in murine mucopolysaccharidosis type VII after syngeneic bone marrow transplantation. *Blood* **78:** 3081–3092.
7. Sands, M. S., *et al.* (1994). Enzyme replacement therapy for murine mucopolysaccharidosis type VII. *J. Clin. Invest.* **93:** 2324–2331.

8. Vogler, C., *et al.* (1997). Murine mucopolysaccharidosis type VII: long term therapeutic effects of enzyme replacement and enzyme replacement followed by bone marrow transplantation. *J. Clin. Invest.* **99:** 1596–1605.
9. Vogler, C., *et al.* (1999). Enzyme replacement in murine mucopolysaccharidosis type VII: neuronal and glial response to β-glucuronidase requires early initiation of enzyme replacement therapy. *Pediatr. Res.* **45:** 838–844.
10. O'Conner, L. H., *et al.* (1998). Enzyme replacement therapy for murine mucopolysaccharidosis type VII leads to improvement in behavior and auditory function. *J. Clin. Invest.* **101:** 1394–1400.
11. Sands, M. S., *et al.* (1993). Treatment of murine mucopolysaccharidosis type VII by syngeneic bone marrow transplantation in neonates. *Lab. Invest.* **68:** 676–686.
12. Vogler, C., Sands, M. S., Levy, B., Galvin, N. J., Birkenmeier, E. H., and Sly, W. S. (1999). Enzyme replacement with recombinant β-glucuronidase in murine mucopolysaccharidosis type VII: impact of therapy during the first six weeks of life on subsequent lysosomal storage, growth, and survival. *Pediatr. Res.* **45:** 838–844.
13. Gao, C., Sands, M. S., Harkins, M. E., and Ponder, K. P. (2000). Delivery of a retroviral vector expressing human β-glucuronidase to liver and spleen decreases lysosomal storage in mucopolysaccharidosis type VII mice. *Mol. Ther.* **2:** 233–244 , doi:10.1006/mthe.2000.0121..
14. Taylor, R. M., and Wolfe, J. H. (1997). Decreased lysosomal storage in the adult MPS VII mouse brain in the vicinity of grafts of retroviral vector-corrected fibroblasts secreting high levels of β-glucuronidase. *Nat. Med.* **3:** 771–774.
15. Taylor, R. M., and Wolfe, J. H. (1994). Cross-correction of β-glucuronidase deficiency by retroviral vector-mediated gene transfer. *Exp. Cell Res.* **214:** 606–613.
16. Marechal, V., Naffakh, N., Danos, O., and Heard, J. M. (1993). Disappearance of lysosomal storage in spleen and liver of mucopolysaccharidosis VII mice after transplantation of genetically modified bone marrow cells. *Blood* **84:** 1358–1365.
17. Moullier, P., Bohl, D., Heard, J. M., and Danos, O. (1993). Correction of lysosomal storage in the liver and spleen of MPSVII mice by implantation of genetically modified skin fibroblasts. *Nat. Genet.* **4:** 154–159.
18. Naffakh, N., Pinset, C., Montarras, D., Li, Z., Paulin, D., and Danos, O. (1996). Long-term secretion of therapeutic proteins from genetically modified skeletal muscles. *Hum. Gene Ther.* **7:** 11–21.
19. Ponder, K. P., *et al.* (2002). Therapeutic neonatal hepatic gene therapy in mucopolysaccharidosis VII dogs. *Proc. Natl. Acad. Sci. USA* **99:** 13102–13107.
20. Zhu, J., Kang, W., Wolfe, J. H., and Fraser, N. W. (2000). Significantly increased expression of beta-glucuronidase in the central nervous system of mucopolysaccharidosis type VII mice from the latency-associated transcript promoter in a nonpathogenic herpes simplex virus type 1 vector. *Mol. Ther.* **2:** 82–94, doi:10.1006/mthe.2000.0093.
21. Wolfe, J. H., Deshmane, S. L., and Fraser, N. W. (1992). Herpesvirus vector gene transfer and expression of β-glucuronidase in the central nervous system of MPS VII mice. *Nat. Genet.* **1:** 379–384.
22. Ghodsi, A., Stein, C., Derksen, T., Martins, I., Anderson, R. D., and Davidson, B. L. (1999). Systemic hyperosmolality improves β-glucuronidase distribution and pathology in murine MPS VII brain following intraventricular gene transfer. *Exp. Neurol.* **160:** 109–116.
23. Ghodsi, A., Stein, C., Derksen, T., Yang, G., Anderson, R. D., and Davidson, B. L. (1998). Extensive β-glucuronidase activity in murine central nervous system after adenovirus-mediated gene transfer to brain. *Hum. Gene Ther.* **9:** 2331–2340.
24. Ohashi, T., Watabe, K., Uehara, K., Sly, W. S., Vogler, C., and Eto, Y. (1997). Adenovirus-mediated gene transfer and expression of human beta-glucuronidase gene in the liver, spleen, and central nervous system in mucopolysaccharidosis type VII mice. *Proc. Natl. Acad. Sci. USA* **94:** 1287–1292.
25. Kosuga, M., *et al.* (2001). Engraftment of genetically engineered amniotic epithelial cells corrects lysosomal storage in multiple areas of the brain in mucopolysaccharidosis type VII mice. *Mol. Ther.* **3:** 139–148 , doi:10.1006/mthe.2000.0234..
26. Kosuga, M., *et al.* (2000). Phenotype correction in murine mucopolysaccharidosis type VII by transplantation of human amniotic epithelial cells after adenovirus-mediated gene transfer. *Cell Transplant.* **9:** 687–692.
27. Kosuga, M., *et al.* (2000). Adenovirus-mediated gene therapy for mucopolysaccharidosis VII: involvement of cross-correction in widespread distribution of the gene products and long-term effects of CTLA-4Ig coexpression. *Mol. Ther.* **1:** 406–413 , doi:10.1006/mthe.2000.0067..
28. Kamata, Y., *et al.* (2001). Adenovirus-mediated gene therapy for corneal clouding in mice with mucopolysaccharidosis type VII. *Mol. Ther.* **4:** 307–312 , doi:10.1006/mthe.2001.0461..
29. Kamata, Y., *et al.* (2003). Long-term normalization in the central nervous system, ocular manifestations, and skeletal deformities caused by a single systemic adenovirus injection into neonatal mice with mucopolysaccharidosis VII. *Gene Ther.* **10:** 406–414.
30. Stein, C. S., *et al.* (2001). In vivo treatment of hemophilia A and mucopolysaccharidosis type VII using nonprimate lentiviral vectors. *Mol. Ther.* **3:** 850–856 , doi:10.1006/mthe.2001.0325..
31. Bosch, A., Perret, E., Desmaris, N., Trono, D., and Heard, J. M. (2000). Reversal of pathology in the entire brain of mucopolysaccharidosis type VII mice after lentivirus-mediated gene transfer. *Hum. Gene Ther.* **11:** 1139–1150.
32. Sferra, T. J., *et al.* (2000). Recombinant adeno-associated virus-mediated correction of lysosomal storage within the central nervous system of the adult mucopolysaccharidosis type VII mouse. *Gene Ther.* **11:** 507–519.
33. Daly, T. M., Okuyama, T., Vogler, C., Haskins, M. E., Muzyczka, N., and Sands, M. S. (1999). Neonatal intramuscular injection with recombinant adeno-associated virus results in prolonged β-glucuronidase expression in situ and correction of liver pathology in mucopolysaccharidosis type VII mice. *Hum. Gene Ther.* **10:** 85–94.
34. Daly, T. M., Vogler, C., Levy, B., Haskins, M. E., and Sands, M. S. (1999). Neonatal gene transfer leads to widespread correction of pathology in a murine model of lysosomal storage disease. *Proc. Natl. Acad. Sci. USA* **96:** 2296–2300.
35. Daly, T. M., Ohlemiler, K. K., Roberts, M. S., Vogler, C., and Sands, M. S. (2001). Prevention of systemic clinical disease in MPSVII mice following AAV-mediated neonatal gene transfer. *Gene Ther.* **8:** 1292–1298.
36. Schultheiss, P. C., Gardner, S. A., Owens, J. M., Wenger, D. A., and Thrall, M. A. (2000). Mucopolysaccharidosis VII in a cat. *Vet. Pathol.* **37:** 502–505.
37. Abreu, S., *et al.* (1995). Growth plate pathology in feline mucopolysaccharidosis VI. *Calcif. Tissue Int.* **57:** 185–190.
38. Simonaro, C. M., Haskins, M. E., and Schuchman, E. H. (2001). Articular chondrocytes from animals with a dermatan sulfate storage disease undergo a high rate of apoptosis and release nitric oxide and inflammatory cytokines: a possible mechanism underlying degenerative joint disease in the mucopolysaccharidoses. *Lab. Invest.* **81:** 1319–1328.
39. Silveri, P., Kaplan, S., Fallon, D., Bayever, E., and August, S. (1991). Hurler syndrome with special reference to histologic abnormalities of the growth plate. *Clin. Orthop.* **269:** 305–311.
40. Arai, Y., *et al.* (1997). Adenovirus vector-mediated gene transduction to chondrocyte: in vitro evaluation of therapeutic efficacy of transforming growth factor-β1 and heat shock protein 70 gene transduction. *J. Rheumatol.* **24:** 1787–1795.
41. Watanabe, S., Imagawa, T., Boivin, G. P., Gao, G., Wilson, J., and Hirsch, R. (2000). Adeno-associated virus vector mediates gene transfer and delivery of chondroprotective IL-4 to murine synovium. *Mol. Ther.* **2:** 147–152 , doi:10.1006/mthe.2000.0111..
42. Gouze, E., *et al.* (2002). In vivo gene delivery to synovium by lentiviral vectors. *Mol. Ther.* **5:** 397–404.
43. Schiller, A. L. (1995). Pathology of Osteoarthritis: Osteoarthritic Disorder (In *K. E. Kunettner, and V. M. Goldgerg, Eds.), pp. 95–101. AAOS, Rosemont.*
44. Wolfe, J. H., and Sands, M. S. (1996). Murine mucopolysaccharidosis type VII: a model system for somatic gene therapy of the central nervous system. *Gene Transfer into Nervous System toward Gene Therapy of Neurological Disorders* (In *P. Lowenstain, and L. Enquist, Eds.), pp.263–274. Wiley, Essex, UK.*

nature
cell biology

MKK7 couples stress signalling to G2/M cell-cycle progression and cellular senescence

Teiji Wada[1,2], Nicholas Joza[1,2], Hai-ying M. Cheng[2], Takehiko Sasaki[2], Ivona Kozieradzki[2], Kurt Bachmaier[2], Toshiaki Katada[3], Martin Schreiber[4], Erwin F.Wagner[5], Hiroshi Nishina[3] and Josef M. Penninger[1,2,6]

During the development of multicellular organisms, concerted actions of molecular signalling networks determine whether cells undergo proliferation, differentiation, death or ageing. Here we show that genetic inactivation of the stress signalling kinase, MKK7, a direct activator of JNKs in mice, results in embryonic lethality and impaired proliferation of hepatocytes. Beginning at passage 4–5, *mkk7*$^{-/-}$ mouse embryonic fibroblasts (MEFs) display impaired proliferation, premature senescence and G2/M cell cycle arrest. Similarly, loss of c-Jun or expression of a c-JunAA mutant in which the JNK phosphorylation sites were replaced with alanine results in a G2/M cell-cycle block. The G2/M cell-cycle kinase CDC2 was identified as a target for the MKK7–JNK–c-Jun pathway. These data show that the MKK7–JNK–c-Jun signalling pathway couples developmental and environmental cues to CDC2 expression, G2/M cell cycle progression and cellular senescence in fibroblasts.

Mitogen-activated protein kinases (MAPKs) are a family of serine/threonine kinases that transduce signals from the cell membrane to the nucleus in response to a wide range of stimuli[1–7]. Two independent stress kinase signalling pathways — p38-MAPK and JNKs (c-Jun *N*-terminal kinase or SAPKs, stress-activated protein kinases) — participate in many different intracellular signalling pathways that control a spectrum of cellular processes, including cell growth, differentiation, transformation and apoptosis[1–7]. Both JNK-activation kinases — MKK4 and MKK7 — are required for full activation of JNK[8–10], and genetic inactivation of *mkk4* results in embryonic lethality with a liver defect between embryonic day 10.5 (E10.5) and E12.5 (ref. 11). However, nothing is known about the role of MKK7 in embryogenesis[12].

Here we show that genetic inactivation of MKK7 in mice results in defective hepatocyte proliferation and embryonic lethality. Inactivation of MKK7 in embryonic fibroblasts results in impaired proliferation, a G2/M cell-cycle arrest and premature senescence. The G2/M cell-cycle kinase CDC2 was identified as a molecular target for MKK7–JNK signalling. Loss of c-Jun or a expression of c-JunAA mutant in which the JNK phosphorylation sites were inactivates[13,14] also resulted in defective G2/M cell cycle progression and impaired CDC2 expression.

Table 1 Embronic lethality in *mkk7*$^{-/-}$ mice

	Litters	*mkk7*$^{+/+}$	*mkk7*$^{+/-}$	*mkk7*$^{-/-}$	Dead (%)	Total
E9.5	2	4	11	2	0 (0)	17
E10.5	2	5	8	5	0 (0)	18
E11.5	26	55	106	47	15 (31.1)	208
E12.5	**16**	**31**	**67**	**33**	**30 (90.9)**	131
E13.5	5	11	17	12	12 (100)	40
E16.5	1	3	4	0	–	7
1W	5	9	21	0	–	39

Embryos were isolated at the indicated time of gestation, analysed for viability and processed for histological staining. Genotypes of embryos were determined by PCR. Viability of embryos was determined by observing heart beating. E = embryonic day; 1W = 1 week after birth.

[1]IMBA (Institute of Molecular Biotechnology of the Austrian Academy of Sciences), c/o Dr. Bohrgasse 3-5, A-1030 Vienna, Austria. [2]University Health Network, Departments of Medical Biophysics and Immunology, University of Toronto, 620 University Avenue, Ontario M5G 2C1, Toronto, Canada. [3]Department of Physiological Chemistry, Graduate School of Pharmaceutical Sciences, University of Tokyo, 7-3-1 Hongo, Bunkyo-ku, 113-0033 Tokyo, Japan. [4]University of Vienna School of Medicine, Dept of Obstetrics and Gynecology Waehringer Guertel 18-20, A-1090 Vienna, Austria. [5]IMP (Research Institute of Molecular Pathology), Dr. Bohrgasse 7, A-1030 Vienna, Austria.
[6]Correspondence should be addressed to J.P. (e-mail: josef.penninger@oeaw.ac.at)

Published online: 22 February 2004; DOI: 10.1038/ncb1098

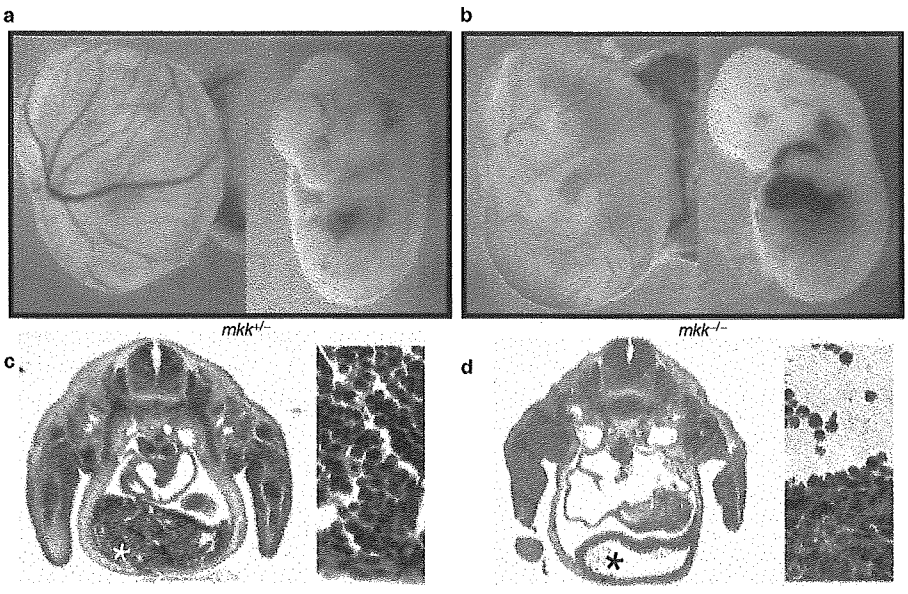

Figure 1 Impaired liver development in *mkk7*$^{-/-}$ embryos. (**a**, **b**) Macroscopic analysis of E11.5 *mkk7*$^{+/-}$ (**a**) and E11.5 *mkk7*$^{-/-}$ (**b**) littermate embryos. (**c**, **d**) Transverse sections of E11.5 *mkk7*$^{+/-}$ (**c**) and E11.5 *mkk7*$^{-/-}$ (**d**) embryos stained with H&E. Note the severe anaemia (**b**) and reduction of parenchymal hepatocytes in E11.5 *mkk7*$^{-/-}$ embryonic livers (asterisk in **c** and **d**). It should be noted that the liver structure and liver parenchyma are overtly normal in E9.5. Right panels show embryonic livers at higher magnifications (×100).

Table 2 Increased G2/M boundaries in *junAA* and *c-Jun*$^{-/-}$ MEFs

Passages	2			4			6			
	mkk7$^{+/-}$	*mkk7*$^{-/-}$	*junAA*	*mkk7*$^{+/-}$	*mkk7*$^{-/-}$	*junAA*	*mkk7*$^{+/-}$	*mkk7*$^{-/-}$	*junAA*	*c-jun*$^{-/-}$
G1 (%)	66.5	70.2	64.0	65.0	56.3	66.9	65.4	64.8	64.6	62.9
S (%)	14.7	11.8	14.5	16.3	13.0	5.8	14.9	9.0	6.4	7.9
G2/M (%)	18.8	18.0	21.5	18.7	**30.3**	**27.3**	19.7	**26.2**	**29.0**	**29.2**

Cells were stained with PI, and cycle profiles were determined in *mkk7*$^{+/-}$, *mkk7*$^{-/-}$, *mkk7*$^{-/-}$, *c-jun*$^{-/-}$ and *c-junAA* MEFs at the indicated passage numbers. Data from one representative experiment are shown.

RESULTS

Generation of *mkk7* knockout mice

The *mkk7* gene was targeted, as shown in Supplementary information Fig. S1a. Disruption of the gene was confirmed by southern blot analysis of genomic DNA and Northern blot analysis of total RNA (see Supplementary Information, Fig. S1b, c). *mkk7*$^{+/-}$ mice appear normal, are fertile, and show no obvious defects. However, no *mkk7*$^{-/-}$ mice were found from intercrosses between heterozygous mice (Table 1). Thus, loss of MKK7 results in embryonic lethality.

MKK7 controls embryonic liver development

To determine the gestational time of *mkk7* lethality, we examined embryos from heterozygous intercrosses at different developmental stages. *Mkk7*$^{-/-}$ embryos died between E11.5 and E13.5 (Table 1). All *mkk7*$^{-/-}$ embryos were severely anaemic, but otherwise normal in appearance (Fig. 1b). PECAM-1 staining of endothelial cells and H&E (haematoxylin and eosin) staining of blood islands from E8.5–E10.5 embryos showed that MKK7 expression is not essential for blood-island formation in the yolk sac and vasculogenesis (data not shown).

Histological analysis revealed that the liver anlage form normally in E8.5 and E9.5 *mkk7*$^{+/+}$, *mkk7*$^{+/-}$, and *mkk7*$^{-/-}$ embryos (data not shown). However, livers from E11.5 and E12.5 *mkk7*$^{-/-}$ embryos were severely disorganized and contained significantly reduced numbers of parenchymal hepatocytes (Fig. 1d). At E11.5 of embryogenesis, the expression levels of p53, MDM2, phospho-ERKs and phospho-p38 seemed comparable between *mkk7*$^{+/-}$ and *mkk7*$^{-/-}$ livers, as well as in whole embryos (see Supplementary information, Fig. S1d). These data show that MKK7 is essential for liver formation during embryogenesis.

Decreased proliferation and premature senescence in *mkk7*$^{-/-}$ MEFs

As genetic inactivation of *mkk7* resulted in embryonic lethality, we analysed the role of MKK7–JNK signalling in MEFs isolated from *mkk7*$^{+/+}$, *mkk7*$^{+/-}$ and *mkk7*$^{-/-}$ embryos. As predicted from other stud-

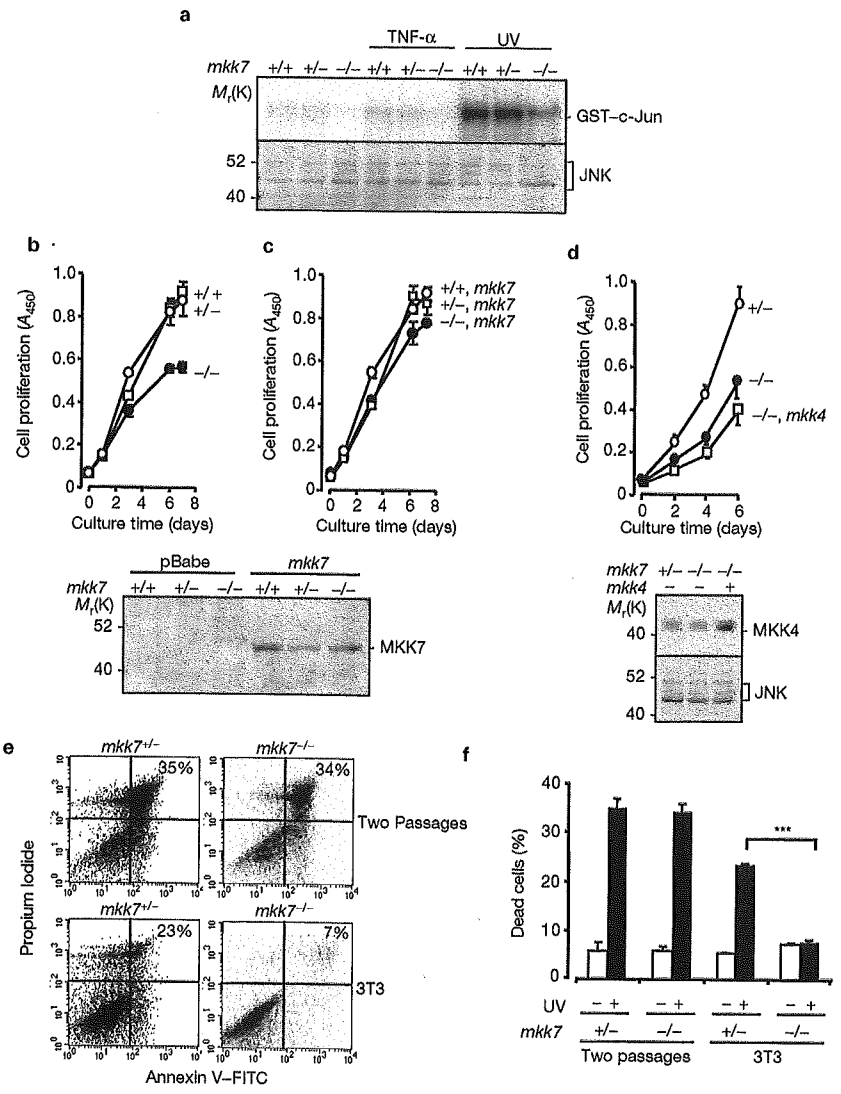

Figure 2 Decreased proliferation and premature senescence of *mkk7*$^{-/-}$ MEFs. (**a**) JNK activity in serum-starved (0.5% serum for 3 days) *mkk7*$^{+/+}$, *mkk7*$^{+/-}$ and *mkk7*$^{-/-}$ MEFs (passage 3) stimulated with TNF-α (10 ng ml^{-1}) and UV (10 J m^{-2}). JNK activity was determined by immune-complex kinase assay using GST–c-Jun as a substrate. (**b–d**) Decreased proliferation of *mkk7*$^{-/-}$ MEFs (passage 4; **b**), and reversal of the proliferation defect by ectopic expression of wild-type MKK7 (**c**), but not by over-expression of wild-type MKK4 (**d**). pBabe (control, **b**), pBabe-MKK7 (**c**) and pBabe-MKK4 (**d**) were introduced into MEFs, and proliferation was determined at the indicated times. Western blots show expression levels of each protein after infection (for the whole blots of **a**, **c** and **d**, see Supplementary information, Fig. S2c–e). In **b**, $P < 0.01$ between *mkk7*$^{+/+}$ or *mkk7*$^{+/-}$ and *mkk7*$^{-/-}$ MEFs (Students *t*-test). (**e**, **f**) Apoptosis in *mkk7*$^{+/-}$ and *mkk7*$^{-/-}$ MEFs. Passage-2 MEFs and 3T3 MEFs were left untreated or were irradiated with 10 J m^{-2} UV 24 h before determination of cell death by annexinV/PI staining. Quantification of three different assays (**f**) and typical annexinV/PI FACS profiles of UV-irradiated MEFs (**e**) are shown. ***$P < 0.001$ between UV-treated *mkk7*$^{+/-}$ and *mkk7*$^{-/-}$ MEFs (Student's *t*-test). In all figures, error bars are shown as standard error of the mean (s.e.m.).

ies[15], loss of MKK7 expression resulted in impaired JNK activation in MEFs at the basal level and after stimulation with tumour necrosis factor α (TNF-α) or UV irradiation (Fig. 2a). Activation and expression of p38-MAPK in MEFs were unaffected in *mkk7*$^{-/-}$ MEFs (data not shown). During the first three passages, cell proliferation was comparable between *mkk7*$^{+/+}$, *mkk7*$^{+/-}$ and *mkk7*$^{-/-}$ MEFs (data not shown). From passages 4–5 onwards, all *mkk7*$^{-/-}$ MEFs analysed showed significantly reduced proliferation under baseline culture conditions (Fig. 2b) and after serum stimulation (data not shown). In all experiments, *mkk7*$^{+/-}$ MEFs behaved similarly to *mkk7*$^{+/+}$ MEFs. Re-expression of wild-type MKK7 (Fig. 2c) restored the reduced proliferation of *mkk7*$^{-/-}$ MEFs to levels observed in wild-type MEFs. Consistent with recent data showing that both MKK4 and MKK7 are required to synergistically activate JNKs[8–10], overexpression of the second JNK activating kinase, MKK4, could not substitute for the loss of MKK7 (Fig. 2d).

To test whether the reduced proliferation in *mkk7*$^{-/-}$ MEFs was

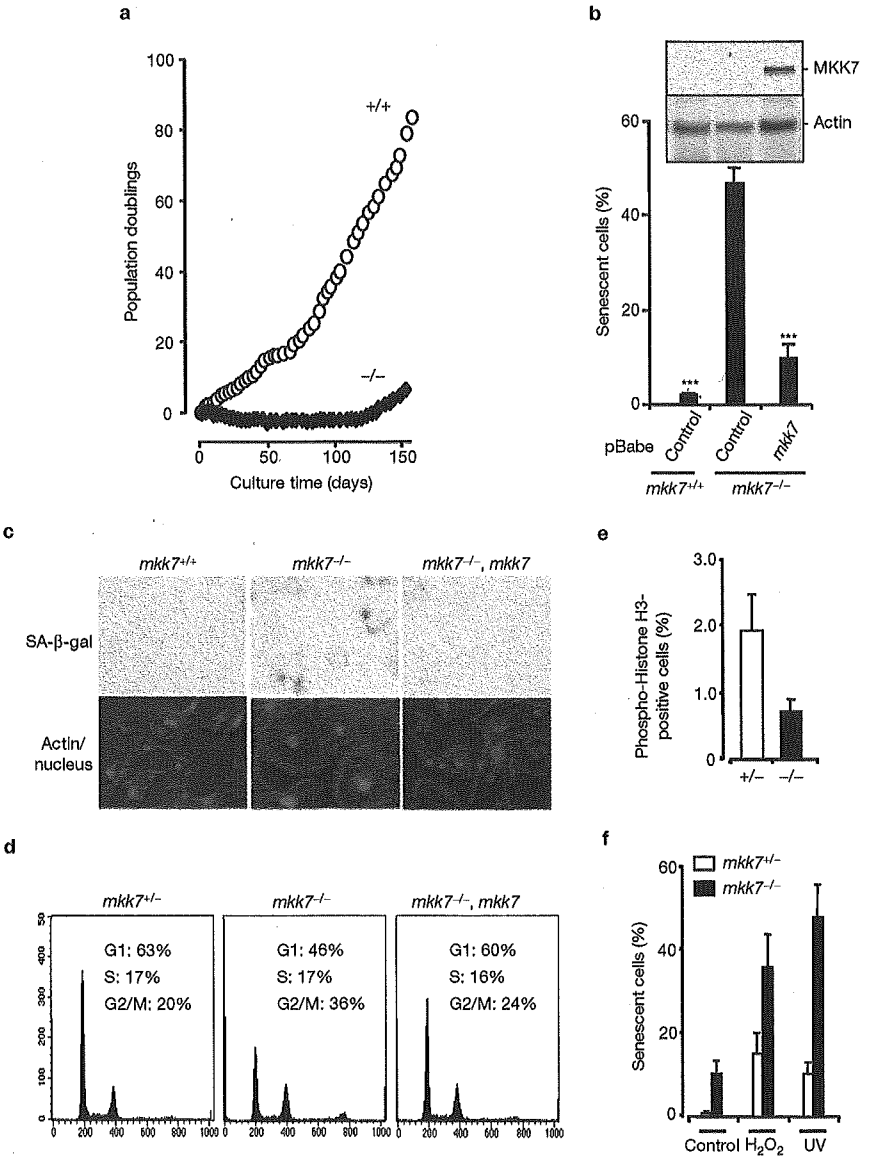

Figure 3 MKK7 is required to protect cells from premature senescence. (**a**) Typical growth curves of *mkk7*$^{+/+}$ and *mkk7*$^{-/-}$ MEFs. One representative experiment out of five is shown. (**b**) Senescence in *mkk7*$^{+/+}$ and *mkk7*$^{-/-}$ MEFs infected with empty pBabe vector (controls) or wild-type MKK7. Senescence was determined at passage 5 by SA-β-galactosidase staining. Western blots show expression levels of each protein after infection (for whole blots, see Supplementary Information, Fig. S2f). ***$P < 0.001$ versus *mkk7*$^{-/-}$ MEFs infected with control pBabe. (**c**) Microscopic analysis of *mkk7*$^{+/+}$, *mkk7*$^{-/-}$ and *mkk7*$^{-/-}$ MEFs expressing wild-type MKK7. SA-β-galactosidase staining (SA-β-gal) is shown in top panels. In the bottom panels, phalloidin–rhodamine (red) was used to stain actin and DAPI (blue) was used to stain nuclei. Representative data from passage-5 cells are shown. Note the flattened and rounded shapes of *mkk7*$^{-/-}$ fibroblasts characteristic of senescent cells. (**d**) Increased G2/M boundaries in *mkk7*$^{-/-}$ MEFs (passage 5) that can be rescued by ectopic expression of wild-type MKK7, but not kinase-dead MKK7 (data not shown). Typical PI FACS analysis is shown for passage-5 MEFs. Some of the *mkk7*$^{-/-}$ cells seem to have greater than 4N DNA content, although this is not a consistent result. (**e**) Numbers of phosphorylated Histone H3-positive cells in *mkk*$^{+/-}$ and *mkk7*$^{-/-}$ MEFs (passage 5) using phospho-specific anti-Histone H3 (Ser10) antibodies. Mean values from three independent experiments are shown. (**f**) *mkk7*$^{+/-}$ and *mkk7*$^{-/-}$ MEFs (passage 3) were UV-irradiated (10 J m^{-2}) or treated with H_2O_2 (150 μM). Stress-induced senescence (mean numbers of SA-β-galactosidase-positive cells) was determined 3 days after stress. The senescent phenotype was confirmed by examination of cell morphology. In addition, increased numbers of cells at the G2/M boundary were observed in those cells (data not shown).

caused by cell-cycle arrest and/or enhanced apoptosis, we first analysed the susceptibility of *mkk7*$^{-/-}$ and *mkk7*$^{+/-}$ MEFs to death stimuli. In particular, it has been shown previously that inactivation of the JNK pathway in MEFs results in resistance to UV-induced cell death[16,17]. Early passage *mkk7*$^{+/-}$ and *mkk7*$^{-/-}$ MEFs showed comparable levels and kinetics of cell death in response to UV- or γ-irradiation (Fig. 2e, f

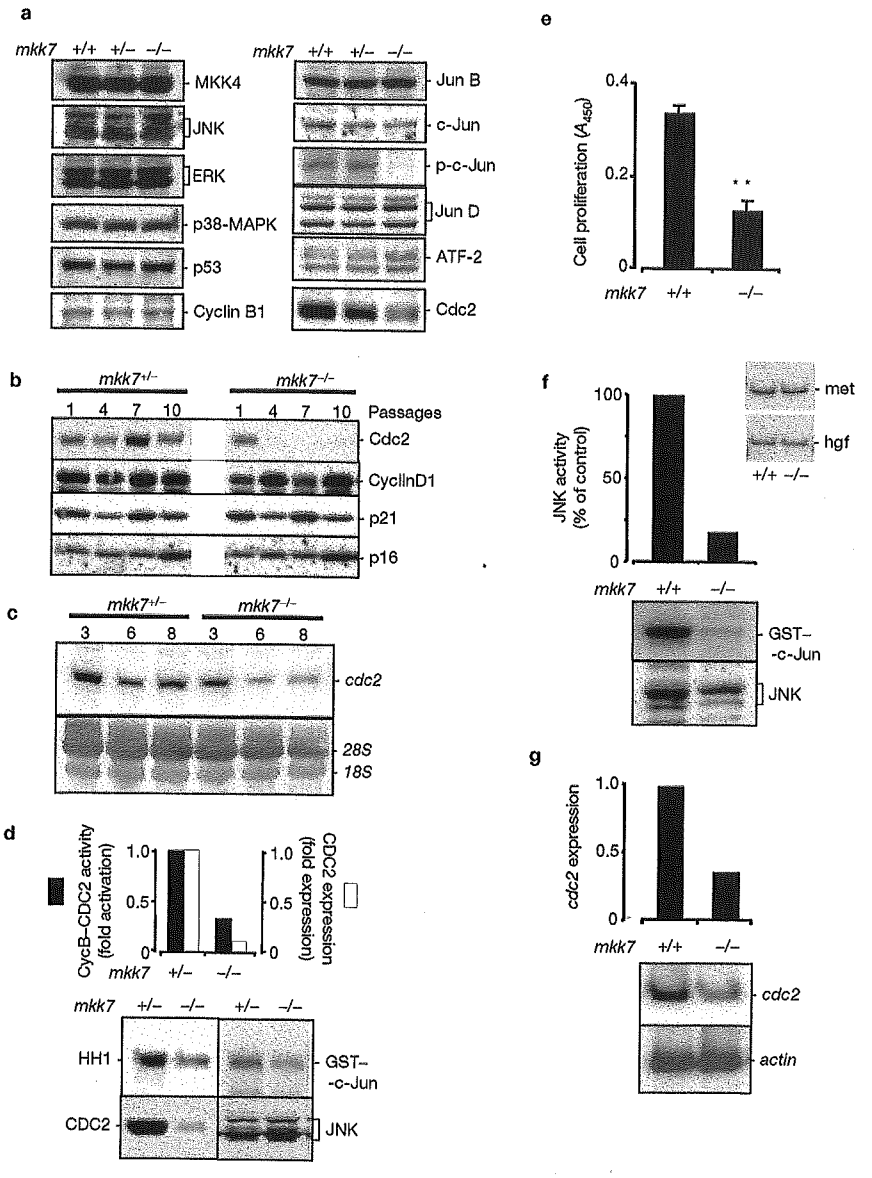

Figure 4 Loss of MKK7 results in decreased CDC2 expression and reduced CDC2 kinase activity. (**a**) Expression levels of the indicated signalling and cell cycle molecules were determined by western blotting of passage-4 *mkk7*$^{+/+}$, *mkk7*$^{+/-}$ and *mkk7*$^{-/-}$ MEFs under normal culture conditions. (**b**) Expression levels of CDC2, cyclinD1, p16 and p21 in passage-1, -4, -7 and -10 *mkk7*$^{+/-}$ and *mkk7*$^{-/-}$ MEFs. (**c**) Reduced expression level of *cdc2* mRNA in *mkk7*$^{-/-}$ MEFs (passage 3, 6 and 8). Total RNA, stained with methylene blue, is shown in the lower panel. (**d**) Decreased cyclin B1–CDC2 complex kinase activity in *mkk7*$^{-/-}$ MEFs (passage 5). CDC2 kinase and JNK activities were determined using Histone H1 (HH1) and GST–c-Jun as substrates. (**e**) Proliferation of embryonic hepatocytes (3×10^3 cells per well) isolated from E11.5 *mkk7*$^{+/-}$ and *mkk7*$^{-/-}$ littermate embryos. $^{**}P < 0.01$. (**f**) Impaired JNK activation in hepatocytes purified from E11.5 *mkk7*$^{-/-}$ embryos. Hepatocytes were stimulated with HGF (30 ng ml^{-1}) for 15 min and then JNK activity was determined by immune-complex kinase assays. Insets show normal levels of *c-Met* and *HGF* mRNA expression in *mkk7*$^{-/-}$ liver cells. (**g**) Decreased expression of *cdc2* mRNA in hepatocytes from E11.5 *mkk7*$^{-/-}$ embryos. Embryonic hepatocytes were isolated as in **e** and quantitative RT–PCR was performed with α-^{32}P-dCTP. PCR products were detected with a phosphoimager. For the whole blots of **a**–**d**, **f** and **g**, see Supplementary Information, Figs S3a–d and 4a, b.

and not shown). Moreover, spontaneous cell death was comparable between the two genotypes at early passages. However, at later times of culture, *mkk7*$^{-/-}$ 3T3 cells showed resistance to UV-irradiation induced cell death (Fig. 2e, f). Our results indicate that the 'history' and passage number of cells is a critical determinant for cell death susceptibility in the absence of MKK7 expression. Importantly, our data show that